



Science Forum (Journal of Pure and Applied Sciences)

journal homepage: <https://atbu.edu.ng/science-forum/>



Subsurface Modelling Of Groundwater Potential Employing GIS Remote Sensing And Electrical Resistivity Within Bayero University New Campus

Ahmed AbubakarSarki¹, Umar Nasiru Umar² and Farouq Mohammed Jibril³, Abdullahi Suleiman Arabi¹

¹Department of Geology Faculty of Earth and Environmental Sciences, Bayero University Kano, Nigeria

²Department of Environmental Management Faculty of Earth and Environmental Sciences, Bayero University Kano, Nigeria

³Division of Agricultural collages Ahmadu Bello University Zaria, Kaduna Nigeria

ABSTRACT

Investigation of groundwater potential zones using GIS, Remote sensing and Resistivity methods is a comprehensive approach that combines geospatial techniques with geophysical surveys, for better understanding of subsurface water availability and distribution. This study combined geospatial techniques with geophysical survey for investigation of ground water potential zones within Bayero University New campus, Kano. The geospatial techniques were conducted using GIS and remote sensing which analyzed the land surface characteristics and hydrological features. Satellite image was used in obtaining the Land use, Land cover as well as the surface water bodies. Potential recharge areas and groundwater flow paths were identified using GIS. Geophysical survey was conducted using electrical resistivity method, by employing Vertical Electrical Sounding (VES). This method was used in mapping out the subsurface groundwater conditions. The results obtained from GIS and Remote sensing produces a groundwater potential maps which was classified into three zones (high potential, moderate potential and low potential). The results obtained from the resistivity methods showed that VES P1, P9 and P22 are within a high potential zone, VES P8, P4 and P30 are within a moderate potential zone and VES P6, P7, P15, P21 and P26 are within a low potential zone which is in agreement with geospatial results. The study area is classified into six (6) lithologic layers which involved the Lateritic sand/Topsoil, laterite, clay sand, weathered basement, Fractured basement and Fresh basement with thickness and depth ranging from 17.72m to 33.65m and 17.72m to 110m. The results showed a strong correlation between the geospatial and geophysical methods.

ARTICLE INFO

Received 22 April 2023

Received in Revised Form 08 May 2023

Accepted 24 May 2023

Published 23 July 2023

Available Online 02 September 2023

KEYWORDS

Remote Sensing, Resistivity, GIS, Vertical Electrical Sounding

Introduction

Water is one of the most essential commodities for mankind and the largest available source of fresh water lays underground. Groundwater plays a crucial role in meeting the water demands of human activities, agricultural practices and industrial processes. Rapid population growth, urbanization, industrialization and agricultural expansion directly translates to an increased demand for water (Chawla et al. 2010). As the

surface water sources become more limited and vulnerable to pollution, societies increasingly rely on groundwater to supplement their water needs.

Consequently, the escalating population exerts considerable stress on groundwater reserves. This can lead to over extraction of groundwater, causing depletion of aquifers. Over-pumping can create a negative balance between recharge rates and extraction, resulting in falling water tables

*Corresponding Author A. A. Sarki ✉ aasarki.geo@buk.edu.ng ✉ Department of Geology Faculty of Earth and Environmental Sciences, Bayero University Kano, Nigeria

and drying wells. This not only affects the availability of water for immediate use but also poses a long-term threat to sustainable groundwater supply (Rao, 2006).

However, through technological advancement we can achieve a balance between population growth and sustainable groundwater exploration. The most effective approach that can be used in achieving this balance is the geospatial method, by integrating GIS and remote sensing.

The use of GIS and remote sensing in identifying groundwater potential zones is of paramount importance for effective and sustainable water resource management. These technologies offer valuable tools for analyzing and visualizing spatial data, enabling scientists, hydro geologists and policy makers to make informed decisions regarding groundwater exploration and utilization (Pathak 2017).

Rahmati et al. (2014) integrated Analytical Hierarchy Process (AHP), GIS and RS technique for mapping groundwater potential at Kurdistan region of Iran. In the study, different thematic layers like rainfall, lithology, drainage density, lineament density and slope percent have been used. The weight for the thematic layers were assigned by eigenvector technique. In the study, rainfall gained the maximum weight, whereas slope percent gained the minimum weight. The validation was done using Receiver Operating Curve (ROC) and found to be fairly good prediction (73.66%).

Bashe (2017) used RS and GIS for groundwater potential mapping in Rift Valley lakes basin of Weito sub basin, Ethiopia. The author used the thematic layers like rainfall, land use, slope, soil, lithology, drainage, lineaments and geomorphic features. Land use and lineaments were extracted from the Landsat 8 OLI/TIRS multispectral images. The weights for the factors were assigned using AHP. The author suggests to use remotely sensed data of higher spatial and spectral resolution for the development of more realistic potential map.

Al-Abadi and Al-Shamma (2014) used AHP and GIS for groundwater potential mapping of the major aquifer in Northeast Missan Governorate, South Iraq. Due to scarcity of data, only four groundwater dependent factors such as geological setting, geomorphologic features, soil

and hydrogeological setting were used. The potential map was verified using the available abstraction rate of existing wells and found the prediction accuracy of 72%.

GIS and remote sensing primarily focus on surface features and land cover. Remote sensing techniques, such as satellite imagery, can sometimes suffer from limitations like cloud cover or sensor resolution. However, Resistivity method serves as an independent and ground-based verification tool for the interpretations derived from Remote sensing data. The resistivity method is an essential technique that complements and validates the findings obtained through GIS and Remote sensing techniques in groundwater exploration and assessment. While GIS and Remote sensing provide valuable spatial data and insights, the resistivity method offers crucial subsurface information, particularly related to the geological and hydrogeological properties. The integration of these three methods enhances the accuracy and reliability of groundwater potential assessments. Geophysical method is one of the most promising techniques that provide an information about the subsurface features of the earth. When combined with geospatial method it provides a precise information about the groundwater potential. This study combines geospatial and geophysical methods to investigate the groundwater potential zones of Bayero University New campus, Kano.

Location and Geology of the Study area

The study area is located in Ungogo local government area along Gwarzo Road of Kano state, in Northern Nigeria and lies between latitudes 8.4102N to 8.4436N and longitudes 11.9617E to 11.984E, Fig 1 which covers an area of about 17.84 km². The study area has the same geology as that of Kano State in general having basement complex mainly. The rock types in the area are older granites, sediment and older basement. The older basement is composed of migmatite, biotite gneiss, and blended gneiss. Joints and fractures in the basement complex rocks are better developed in the granites and quartzite and less in the gneisses and migmatite. (www.kanostate.net, 2019)

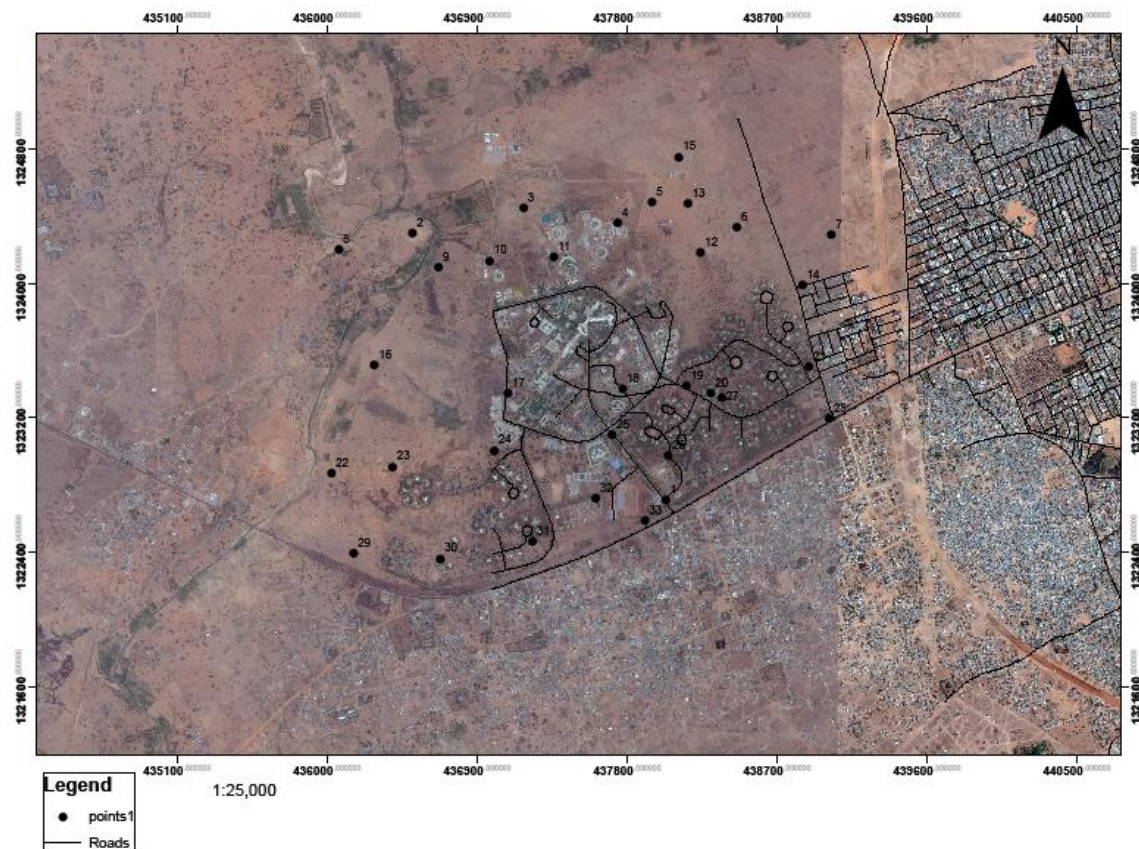


Figure 1: Satellite Image of the study area showing the VES points

Materials and methods

GIS and Remote Sensing

Overlay analysis is a multi-criteria analysis wherein analysis can be carried out with complex things for finding out certain theme with the help of assignment of rank to the individual class of feature and then assigning weight age to the individual feature considering its influence over theme. All the thematic maps were converted into raster format and superimposed by weighted overlay method, which consists of rank and weight age wise thematic maps and integration of them through GIS. Integration of thematic maps for carrying out multi-criteria or overlay analysis in GIS environment was done using Arc GIS 10.8.2 software. Fig 3& 6

Electrical Resistivity Method

The survey was conducted using the electrical resistivity method. ABEMT terra meter SAS(1000) was setup with all its accessories in place while choosing twelve (12) profiles along fractured lines upon which four(4) electrodes were driven in to the ground at certain distance enough to allow the flow of current. The cables which supplied the current into the ground were

connected to A and B ports of the machine. The other ends of the wires were fitted with crocodile clips and were fixed in electrode 1 and 4 respectively. Also, the potentials M and N were connected to electrodes 2 and 3 respectively through which the potential difference was measured. A VES point is randomly selected along each profile, which involve P1, P4, P6, P8, P9, P15, P21, P22, P26, P28 and P30 respectively. The Vertical Electrical Sounding (VES) using Schlumberger array configuration was adopted for the survey. A total numbers of 12 VES stations were selected on the twelve profiles Fig 4 & 5 within the electrode spacing varying from 1.5 to 72, 55, 55, 55, 55, 55, 55, 72 and 55m at P1, P4, P6, P8, P9, P15, P21, P22, P26, P28 and P30 respectively with total spread length of 110m. The measurement was carried and data were collected and arranged in a format that is acceptable to a computer program.

Data Analysis and Interpretation

The data were acquired by profiling mode with increase in spacing along twelve (12) profiles. The collected data was clean, smoothed and modeled producing resistivity parameter table and corresponding curves' plot. Earth imager 1D software was used to interpret apparent

resistivity field data and to compute the inverse model of resistivity variation with depth. This program has provision of accomplishing three tasks: (i) smoothing of noisy field data, (ii) accurate computation of apparent resistivity models, and (iii) inversion of resistivity data. The output is the inverse resistivity model providing layer wise distribution of resistivity value (ρ) and thickness (h) of the corresponding layer. Data smoothing for Schlumberger array includes single point correction and vertical curve branch

shifting. The vertical curve branch shifting consists of a linear shift to one or more branches to correct mistakes between the branches. The correction of the mistakes is by the amount of the difference between two apparent resistivity observations with the same current electrode distance (AB), Fig 2 but with different potential electrode separation (MN). An equal correction (on the logarithmic scale) is applied to all points of a selected branch.

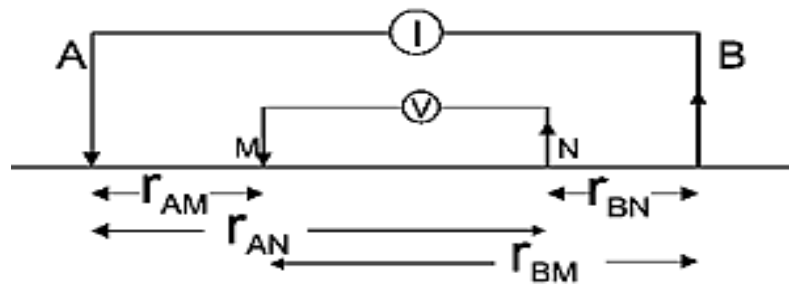


Figure2: Diagram showing the electrical resistivity configuration

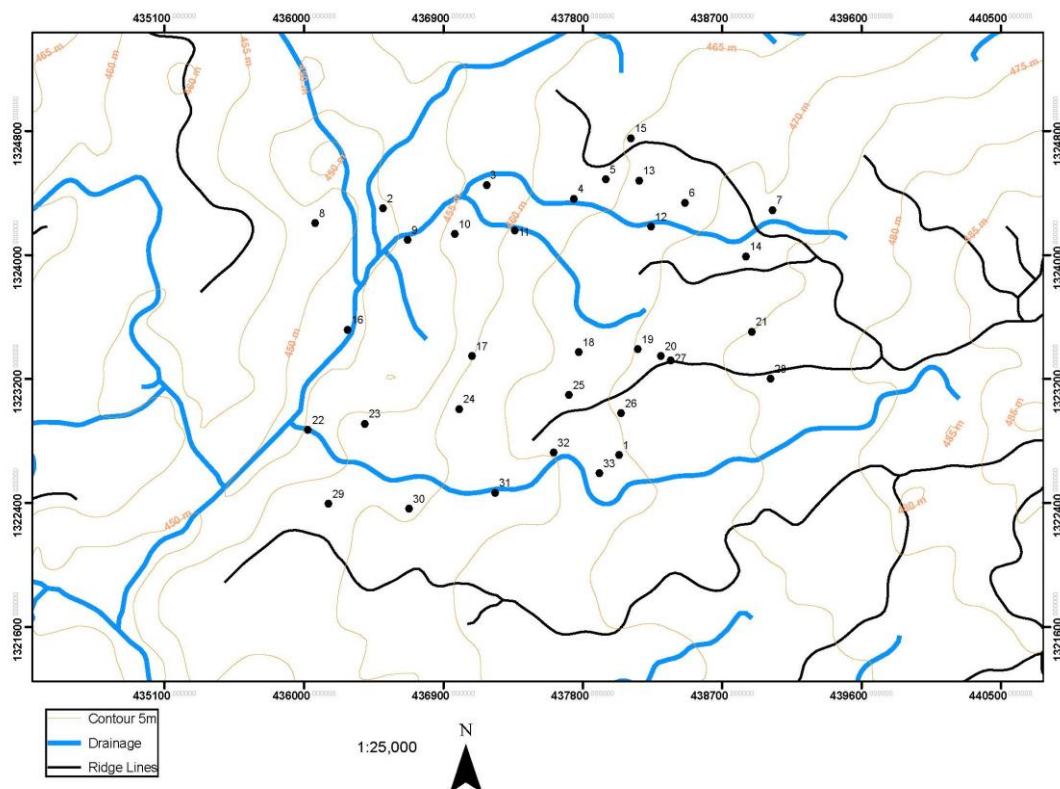


Figure3: Map of the study area showing Contour and Drainage pattern

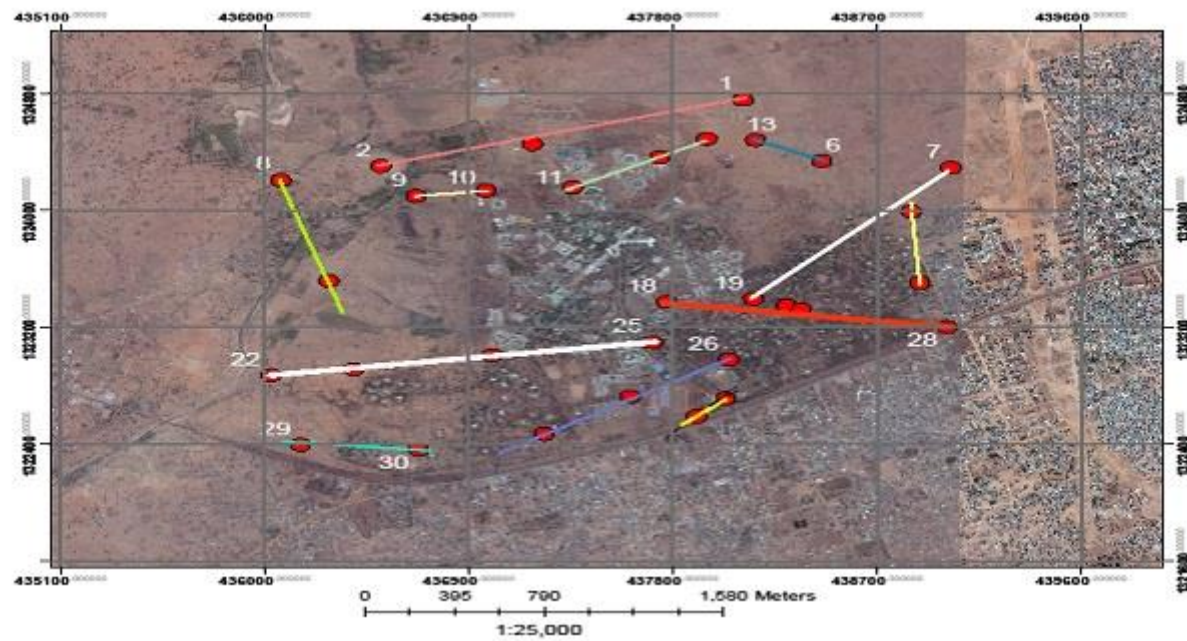


Figure 4: Map of the study area showing the profile lines and the VES points

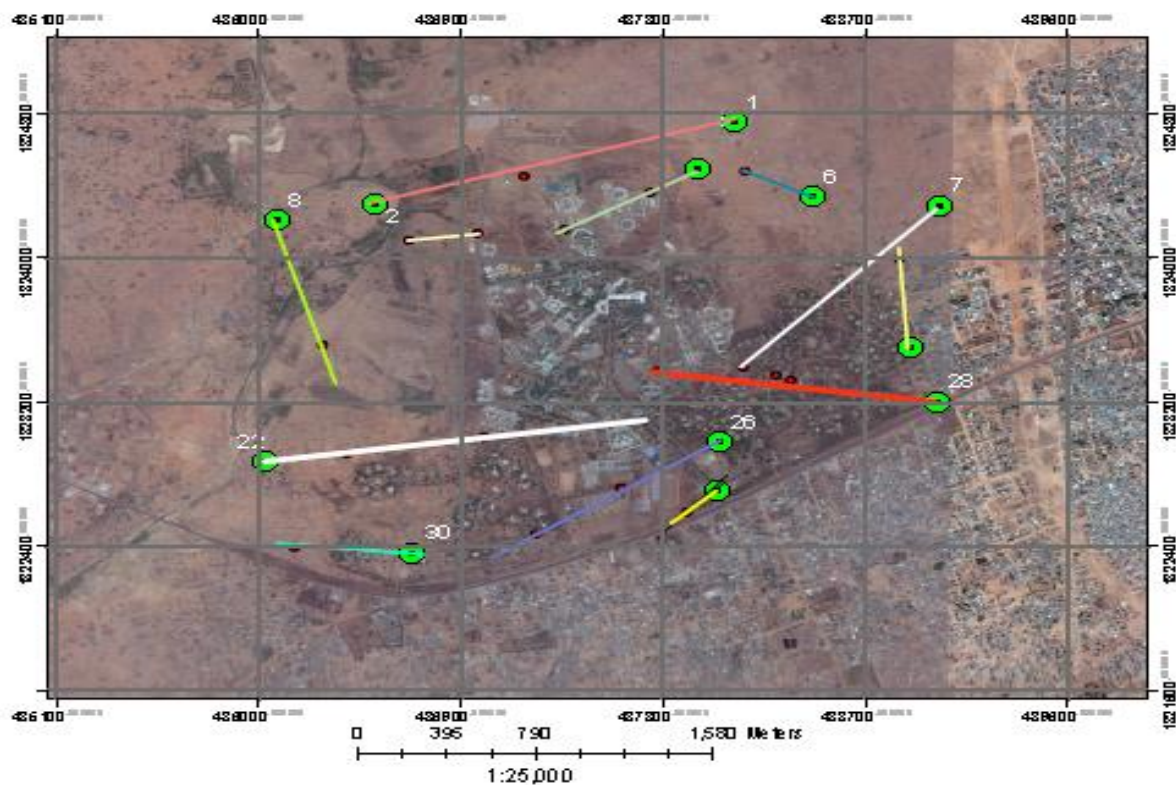


Figure 5: Map showing the selected VES points

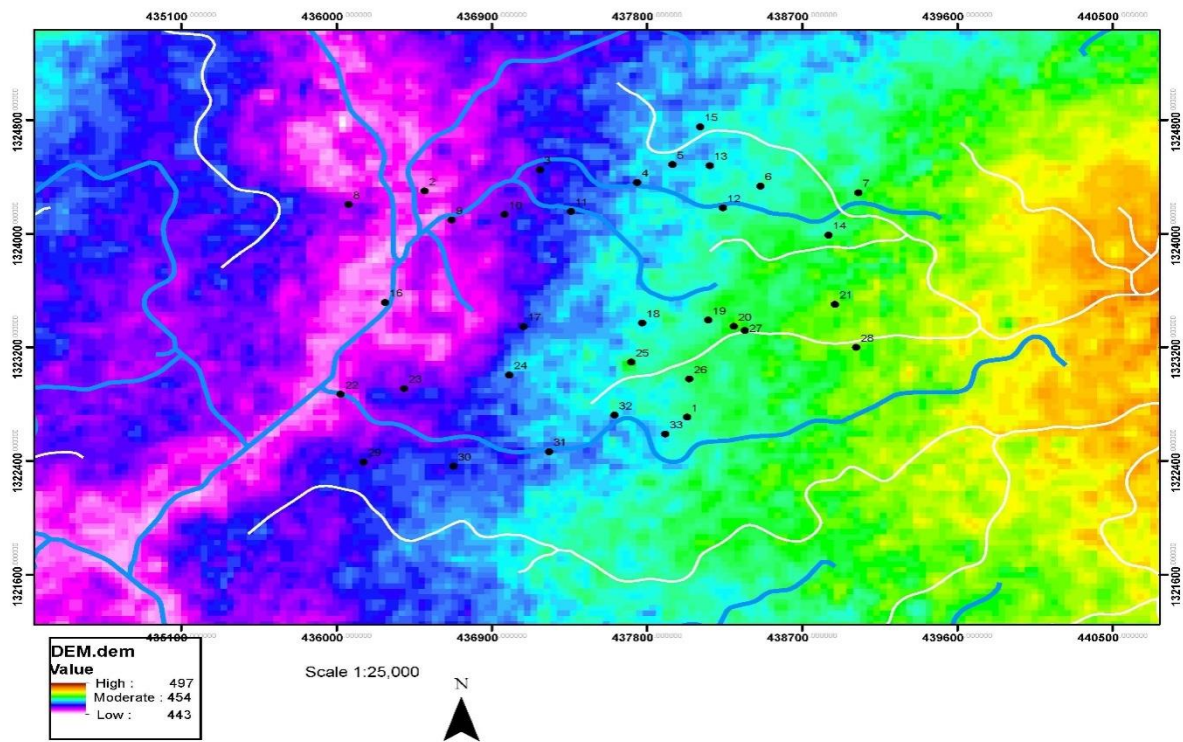


Figure 6: Map showing the Digital Elevation model of the study area

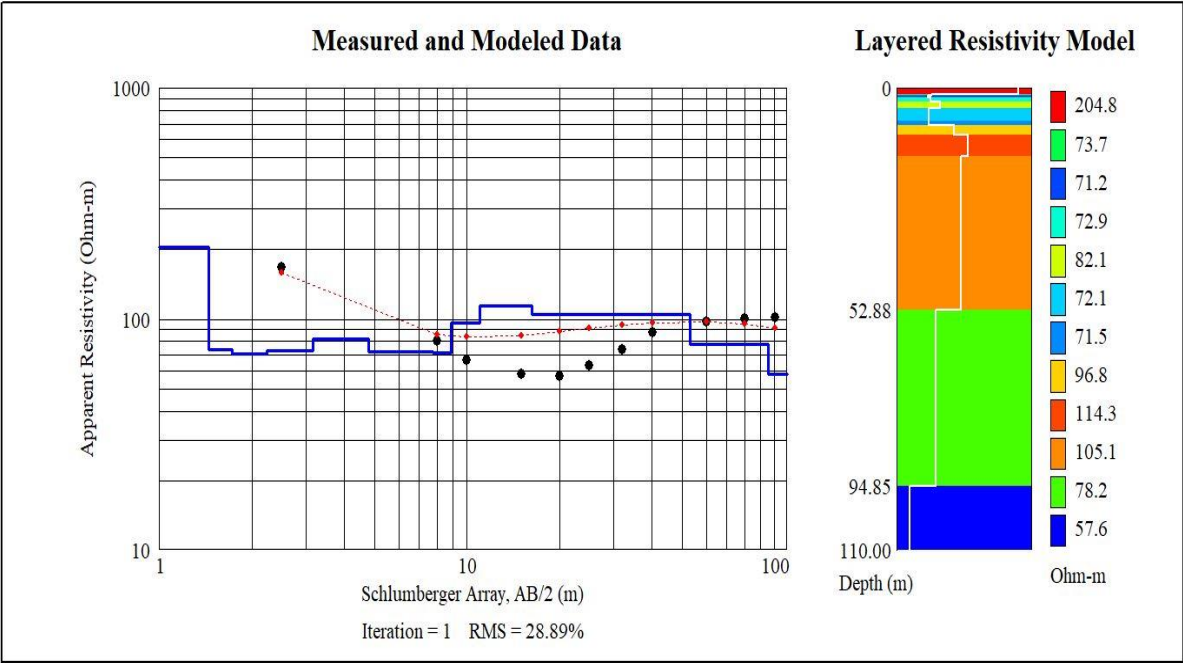


Figure 6: VES1 showing AKA Curve type

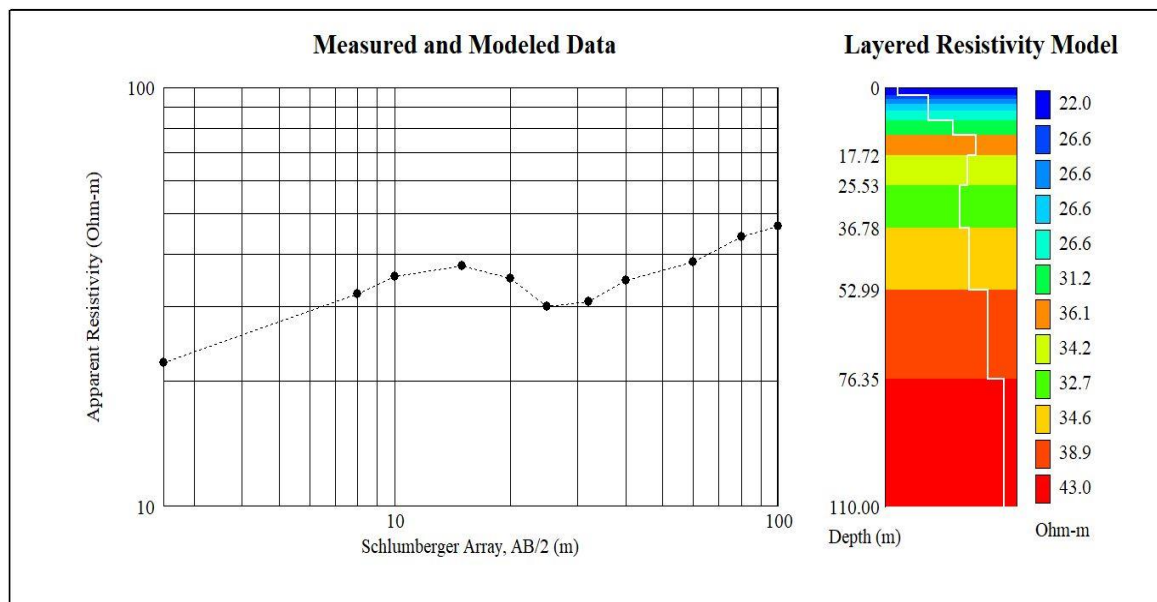


Figure 7: Inverse resistivity model of VES1

Table1: Presents the geoelectrical Stratification for all the VES survey carried out in the study area

VES points	Curve type	Layer no.	Resistivity (Ωm)	Thickness (m)	Depth (m)	Lithology
P1	AKA	1	27.95	17.72	17.72	Laterite /Top soil
		2	34.20	7.81	25.53	Lateritic sand
		3	32.70	11.25	36.78	Clay sand
		4	34.60	16.21	52.99	Clay, silt and sand
		5	38.90	23.36	76.35	Clay, silt and sand
		6	43.00	33.65	110.00	Fractured basement
P4	QHA	1	39.80	17.72	17.72	Top soil
		2	58.40	7.81	25.53	Lateritic sand
		3	70.60	11.25	36.78	Clay sand
		4	82.20	16.21	52.99	Clay sand
		5	87.30	23.36	76.35	Clay, silt and sand
		6	96.20	33.65	110.00	Fractured basement
P6	QHA	1	107.85	17.72	17.72	Weathered basement
		2	27.60	7.81	25.53	Laterite/ top soil
		3	39.00	11.25	36.78	Clay sand
		4	56.30	16.21	52.99	Clay sand
		5	62.70	23.36	76.35	Fractured basement
		6	68.80	33.65	110.00	Fractured basement
P7	AAA	1	47.50	17.72	17.72	Laterite
		2	34.70	7.81	25.53	Lateritic sand
		3	33.60	11.25	36.78	Clay sand
		4	40.40	16.21	52.99	Clay sand
		5	51.00	23.36	76.35	Fractured basement
		6	63.00	33.65	110.00	Fractured basement

P8	AKA	1	94.50	17.72	17.72	Lateritic sand
		2	109.30	7.81	25.53	Weathered basement
		3	92.00	11.25	36.78	Fractured basement
		4	86.50	16.21	52.99	Fractured basement
		5	99.40	23.36	76.35	Fractured basement
		6	128.80	33.65	110.00	Weathered basement
P9	QHA	1	59.00	17.72	17.72	Laterite sand
		2	91.70	7.81	25.53	Fractured basement
		3	97.40	11.25	36.78	Fractured basement
		4	101.60	16.21	52.99	Weathered basement
		5	114.20	23.36	76.35	Weathered basement
		6	121.90	33.65	110.00	Weathered basement
P15	QHA	1	117.90	17.72	17.72	Weathered basement
		2	76.20	7.81	25.53	Lateritic sand
		3	70.00	11.25	36.78	Fractured basement
		4	64.20	16.21	52.99	Fractured basement
		5	69.30	23.36	76.35	Fractured basement
		6	77.00	33.65	110.00	Fractured basement
P21	AKA	1	129.70	17.72	17.72	Lateritic sand
		2	121.90	7.81	25.53	Weathered basement
		3	131.00	11.25	36.78	Fresh basement
		4	140.40	16.21	52.99	Fresh basement
		5	138.10	23.36	76.35	Fresh basement
		6	138.80	33.65	110.00	Fresh basement
P22	AKA	1	58.30	17.72	17.72	Top soil
		2	66.50	7.81	25.53	Clay sand
		3	80.30	11.25	36.78	Fractured basement
		4	100.7	16.21	52.99	Weathered basement
		5	119.7	23.36	76.35	Weathered basement
		6	142.1	33.65	110.00	Weathered basement
P26	AKA	1	302.90	17.72	17.72	Fresh basement
		2	128.5	7.81	25.53	Weathered basement
		3	137.70	11.25	36.78	Weathered basement
		4	160.70	16.21	52.99	Weathered basement
		5	172.90	23.36	76.35	Weathered basement
		6	181.50	33.65	110.00	Weathered basement
P28	QQA	1	116.30	17.72	17.72	Weathered basement
		2	48.00	7.81	25.53	Fractured basement
		3	46.10	11.25	36.78	Fractured basement
		4	49.00	16.21	52.99	Fractured basement
		5	56.40	23.36	76.35	Fractured basement
		6	67.00	33.65	110.00	Fractured basement
P30	AAA	1	76.65	17.72	17.72	Clay sand
		2	97.80	7.81	25.53	Clay sand
		3	110.20	11.25	36.78	Weathered basement
		4	121.80	16.21	52.99	Weathered basement
		5	128.40	23.36	76.35	Weathered basement
		6	130.50	33.65	110.00	Weathered basement

According to Table1 VES P1,P8,P21,P22 and P26 showed an (AKA) Fig 6 shape curve type which is define by a sequence of resistivity $\rho_1 < \rho_2 < \rho_3 > \rho_4$

$< \rho_5$. The inverse resistivity model of the observed curve resolved the penetrating rocks into six (6) geoelectric layers with resistivity values ranging

from $27.95\Omega\text{m}$ to $43.00\Omega\text{m}$ at P1, $94.50\Omega\text{m}$ to $128.80\Omega\text{m}$ at P8, $129.70\Omega\text{m}$ to $138.80\Omega\text{m}$ at P21, $58.30\Omega\text{m}$ to $142.12\Omega\text{m}$ at P22 and $302\Omega\text{m}$ to $181.50\Omega\text{m}$. The depth and thickness of the points ranges from 17.72m to 110m and 7.81m to 33.65m respectively. The resistivity values of P1 and P22 indicates that the points are within a high potential zone, while the resistivity values of P8 indicate that the point is likely to be within a low potential zone and the resistivity values of P21, P26 indicate that the points are within a poor potential zone.

VES points P4, P6, P9 and P15 Fig 8 exhibited a QHA curve type defined by a sequence of resistivity $\rho_1 > \rho_2 > \rho_3 < \rho_4 < \rho_5$. The curve is characterized by five (5) rock types which involved Top Soil, lateritic sand, Clay sand, weathered basement and fractured

basement. Vertical Electrical sounding point P4 showed a flat topography with sandy soil belonging to lateritic terrain, the range of resistivity values $39.80\Omega\text{m}$ to $96.20\Omega\text{m}$ along the point indicates that the point is within a moderate potential zone. Vertical Electrical Sounding points P6 and P15 are dominated by weathered and fractured basement with high resistivity values of 107.85 and 117.90 at the top layers, these high resistivity values implies that the points are within a low potential zone. Point P9 have range of resistivity value which ranges from $59.0\Omega\text{m}$ to $121.90\Omega\text{m}$ which showed a flat topography with lateritic sand followed by a layer underlain by fractured basement and also a layer underlain by weathered basement which deduced that the point is within a high potential.

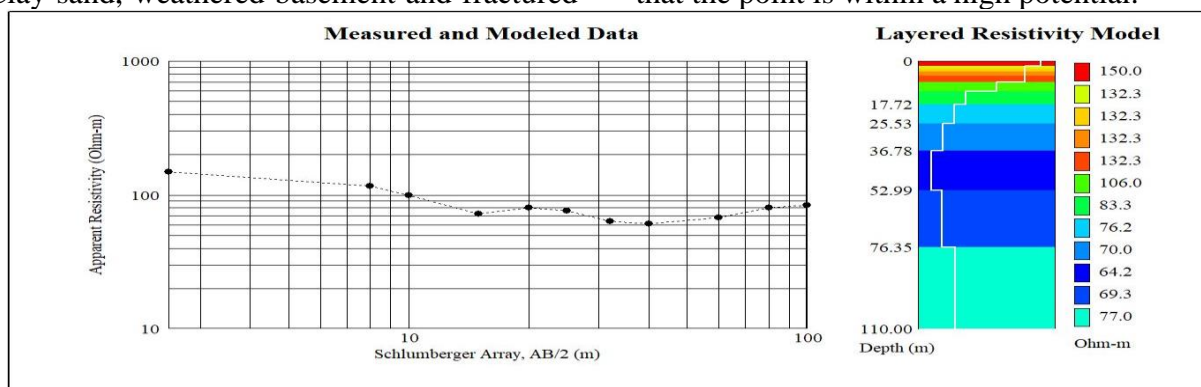


Figure 8: VES15 showing QHA Curve type

VES points P7 and P30 Fig 9 showed (AAA) curve type defined by a sequence of resistivity $\rho_1 < \rho_2 < \rho_3 < \rho_4 < \rho_5$ which corresponds to six subsurface layers which comprises mostly clay sand and weathered basement. VES P7 have a resistivity values ranging from $47.50\Omega\text{m}$ to $51.00\Omega\text{m}$ which are characterized into laterite, clay sand and fractured basement indicating that the point is within a low potential zone. VES P30 have a resistivity values ranging from $76.65\Omega\text{m}$ to

$130.50\Omega\text{m}$ which are characterized six subsurface layers comprises of clay sand in the first and second layers followed by weathered basement in the third, fourth, fifth and sixth layers. The range of resistivity values indicates that the point is within a moderate potential zone.

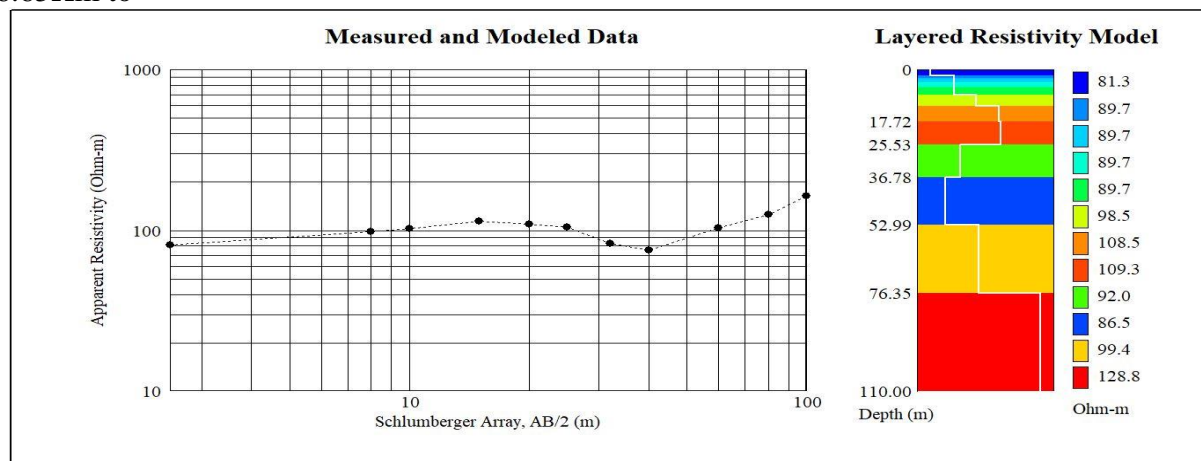


Figure 9: VES7 showing AAA Curve type

VES point P28 exhibited a QQA curve defined by $\rho_1 > \rho_2 > \rho_3 > \rho_4 < \rho_5$. Fig 10 the inverse resistivity modeled of the observed curve resolved the rock type into six lithologic layers. The first layer was interpreted as Weathered basement with resistivity value of $116.30\Omega\text{m}$, followed by the second layer which was interpreted as Fractured basement with resistivity value of $48.00\Omega\text{m}$, the third layer was also

interpreted as Fractured basement with resistivity value $46.10\Omega\text{m}$, the fourth, fifth and sixth layers were also interpreted as Fractured basement which have resistivity values of $49.00\Omega\text{m}$, $56.40\Omega\text{m}$ and $67.00\Omega\text{m}$ respectively. According to the resistivity values the point is within a low potential zone Fig 10.

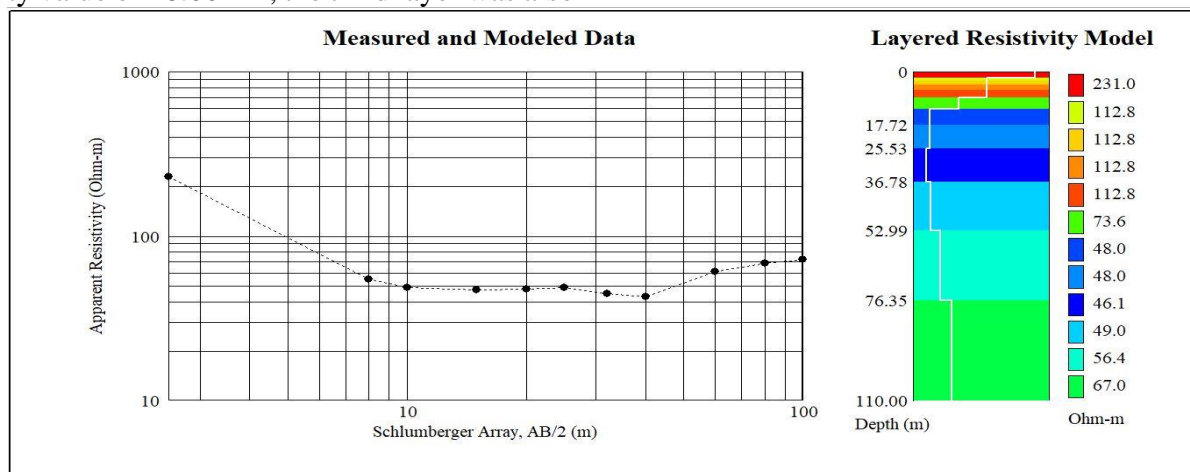


Figure 10: VES28 showing QQA Curve type

Classification of groundwater potential zones

The groundwater potential zones revealed three distinct zones, namely high, low and no potential zones, whose distribution and extents covers the study area, respectively. The prospective map, as presented in Fig 11, gives a swift evaluation of the occurrence of ground water resources in the study area. The groundwater potential map Fig 11 shows that the upper northwestern, the lower southwestern have high potential limited region of central parts of the study area the moderate potential zones covers a larger proportion with the high potential zone at centre of the moderate potential zone extending northwest to southwestern parts while from the northeastern to southeastern and central parts

generally show no potential in a lesser degree. The high to moderate groundwater potential of the study area as shown in fig 11 have higher coverage is a confirmation of good capability as fractured zones within the basement terrain. Moreover, a closer assessment of the groundwater potential map shows that the distribution reflects the patterns of soil in addition to the geological control. High drainage density as well as high and low percentages of slope which can enhance infiltration of water into the groundwater system could be attributed to the observed high potential of groundwater exhibited in the southern parts of the study area

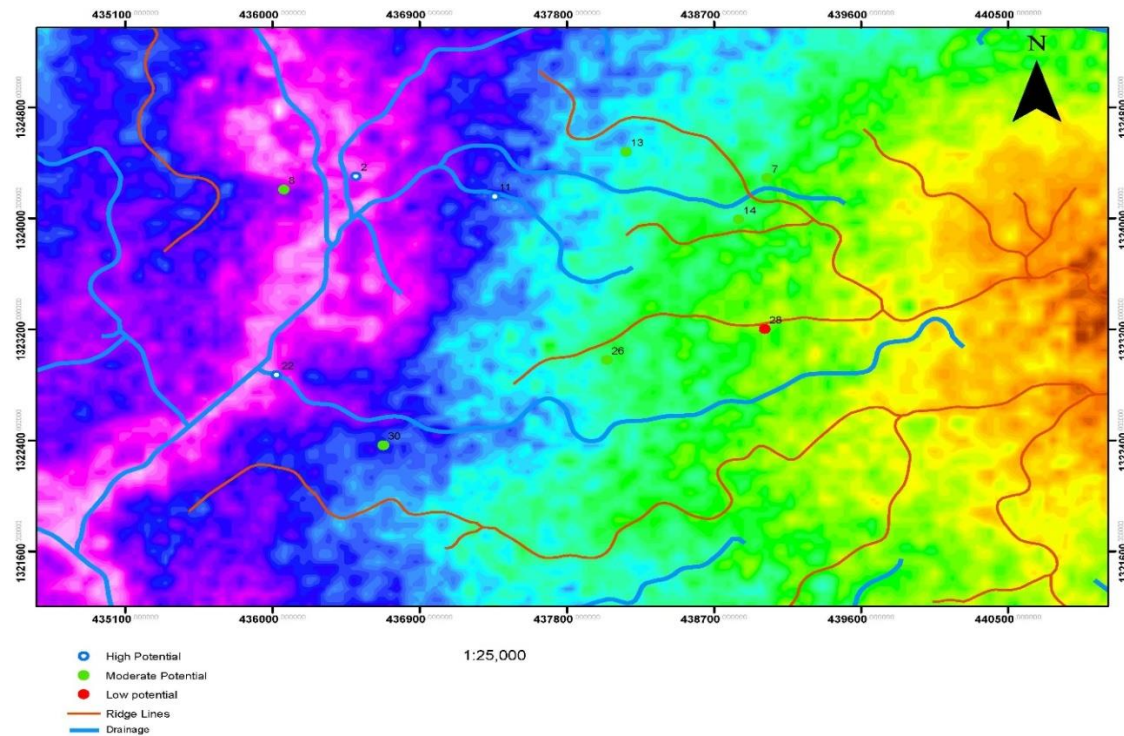


Figure 11: Ground water potential map

Conclusion

This study combined geospatial techniques with geophysical survey for investigation of groundwater potential zones within Bayero University New campus, Kano. The geospatial techniques was conducted using GIS and Remote sensing which analyzed the land surface characteristics and hydrological features. Landsat7 was used in obtaining the Land use, Land cover as well as the surface water bodies. Potential recharge areas and groundwater flow paths were identified using GIS. Geophysical survey was conducted using electrical resistivity method, by employing Vertical Electrical Sounding (VES). This method was used in mapping out the subsurface groundwater conditions. The results obtained from GIS and Remote sensing produces a groundwater potential maps which was classified into three zones (high potential, low potential and no potential). The results obtained from the resistivity methods showed that VES P1, P9 and P22 are within a high potential zone, VES P8, P4 and P30 are within a low potential zone and VES P6, P7, P15, P21 and P26 are within no potential zone which is in agreement with geospatial results. The study area is classified into six(6) lithologic layers which involved the Lateritic sand/Top soil, laterite, clay sand, weathered basement, Fractured basement and Fresh basement with thickness and depth ranging from 17.72m to 33.65m and 17.72m to 110m. The results of the study showed that the

Resistivity method is crucial in validating GIS and Remote Sensing by providing essential subsurface information, confirming groundwater potential zones, and enhancing accuracy of groundwater exploration and assessment. The integration of these methods ensures a comprehensive understanding of the groundwater system, supporting sustainable water resource management and decision making.

Acknowledgments

The authors are grateful to Bayero University Kano and would like to express their sincere appreciation to Directorate for Research Innovation and Partnership (DRIP) for funding the research through TETFUND IBR Fund. Constructive suggestions and comments on the manuscript from the reviewers are very much appreciated.

References

- Al-Abadi, A., and Al-Shamma, A., (2014). Groundwater potential mapping of the major aquifer in northeastern Missan Governorate, south of Iraq by using analytical hierarchy process and GIS. *Jour. Env. Earth Sci.*, v. 4(10), pp. 125–150
- Bashe, B.B., (2017). Groundwater potential mapping using Remote Sensing and GIS in Rift

valley Lakes Basin, Weito sub-Basin, Ethiopia.
Int. Jour. Sci. Engg. Res., v. 8(2), pp. 43–50.

Chawla JK, Khepar SD, Sondhi SK, Yadav AK
(2010). Assessment of long-term groundwater
behaviour in Punjab, India. Water Int 35(1):63–
77

Pathak, D., (2017). Delineation of groundwater
potential zone in the Indo-Gangetic plain
through GIS analysis. Jour. Inst. Sci. Tech., v.
22(1), pp. 104–109.

Rahmati, O., Samani, A.N., Mahdavi, M.,
Pourghasemi, H.R., and Zeinivand, H., (2014).
Groundwater potential mapping at Kurdistan
region of Iran using analytic hierarchy process
and GIS. Arab Jour. Geosci., v. 8(9), pp. 7059–
7071

Rao NS (2006) Groundwater potential index in a
crystalline terrain using remote sensing data.
Environ Geol 50:1067–1076

www.kanostate.net, (2019). *Geology and
Hydrogeology of Kano State*. Retrieved on
20/06/2023 at 1:33PM